Supplementary Information - The EFG Rosetta Stone: Translating between DFT calculations and solid state NMR experiments

Javier Valenzuela Reina,* Federico Civaia*, Angela F. Harper*, Christoph Scheurer* and Simone S. Köcher†*

1 Further Computational Details

1.1 CASTEP v23.1

All EFG calculations are converged with respect to the basis set cut-off energy and the k-point grid by scanning both quantities in steps of 100 eV and 0.01 Å k-point spacing, respectively. The convergence criterion is given by a variation of $\leq$5% in C_Q and η of the nucleus of interest (^{27}Al or ^{7}Li).

As shown in Figure S1, the C_Q and η values converge smoothly at increasing cut-off energies. At 900 eV, we find that all values of C_Q and η are converged below 5%. In order to ensure stable convergence, we chose to use a plane wave cut-off of 1000 eV. We chose to converge C_Q and η directly, as these are the observable quantities that we compare in all reference scales shown in the main text. If we then consider the convergence of V_{xx}, V_{yy}, V_{zz} as shown in the bottom panel of Figure S1, we see that almost all values are converged at a cut-off of 1000 eV. However the V_{xx} values for ^{7}Li in $Li_2B_4O_7$ do not exhibit a smooth convergence due to the small absolute value of V_{xx} for $Li_2B_4O_7$. The range of V_{xx} is from 0.00002 to 0.00040, and therefore the % between subsequent cut-offs is very high. This is also why it is useful to converge η over the individual eigenvalues, as error cancellation between V_{xx} and V_{yy} gives faster convergence.

The geometry optimizations with the Broyden–Fletcher-Goldfarb–Shanno (BFGS) method are conducted with the cut-off energy and k-point grid determined with C_Q convergence. The relaxations are converged with an energy tolerance of 2.0×10^{-5} eV/atom, a maximum force of 0.05 eV/Å, an a stress tolerance of 0.1 GPa/atom.

Unless specified differently, all calculations treat the simulation cell as an electrical insulator, apply all the symmetry operations detected by the code, and use the default on-the-fly (otf) generated ultra-soft PPs for every element. The CASTEP v23.1 default PP for Li is identical to the default PP in CASTEP v19.1 and is hence abbreviated C19. The electronic energy minimization threshold is set to 10^{-5} eV/atom for SCF convergence. When the impact of the PP is tested, the modified PPs are implemented by changing the string passed to the otf PP generator. The EFG calculations use an integration grid three times finer than the standard grid.

1.2 Quantum Espresso 7.2

The same convergence tests as described above are carried out with respect to the cut-off energy in steps of 10 Ry and for the uniform k-point grid in steps of 1, using the same criterion as specified for the CASTEP tests.

The employed PPs are extracted from the Davide Ceresoli set of GIPAW-compatible PPs[133]. The applied .UPF files for each studied atom are listed in S1.

Table S1 GIPAW-compatible PPs from the Davide Ceresoli set used for Quantum ESPRESSO calculations[133]

Atom	PP file
H	H.pbe-rrkjus-gipaw-dc
Li	Li.pbe-paw-gipaw-nh
B	B.pbe-rrkjus-gipaw-dc
C	C.pbe-rrkjus-gipaw-dc
O	O.pbe-rrkjus-gipaw-dc
F	F.pbe-rrkjus-gipaw-dc
Na	Na.pbe-tm-gipaw-dc
Mg	Mg.pbe-tm-gipaw-dc
Al	Al.pbe-tm-gipaw-dc
Si	Si.pbe-tm-new-gipaw-dc
P	P.pbe-tm-new-gipaw-dc
S	S.pbe-tm-gipaw-new-dc
K	K.pbe-tm-semi-gipaw-xy
Ca	Ca.pbe-tm-new-dc
Nb	Nb.pbe-mt-semi-dc

* Fritz-Haber Institute of the Max Planck Society, Berlin (DE)
† Institut für Energie und Klimaforschung (IEK-9), Forschungszentrum Jülich GmbH, Jülich, (DE)

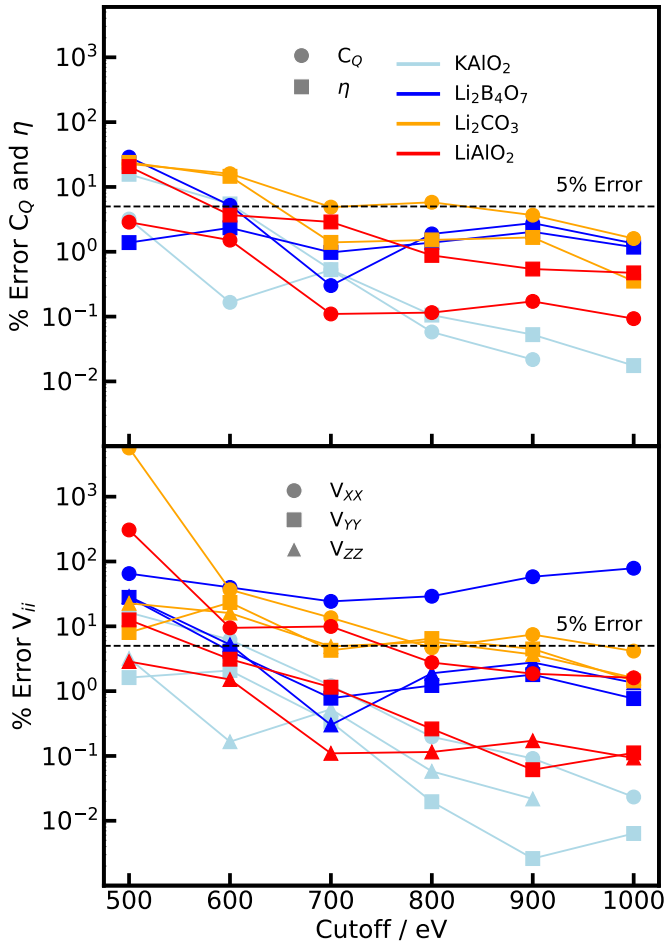

Fig. S1 Convergence of the C_Q and η (top) parameters and the V_{xx}, V_{yy}, V_{zz} eigenvalues (bottom). Convergence is calculated for two Li compounds ($Li_2B_4O_7$ and Li_2CO_2) and two Al containing compounds (γ-$LiAlO_2$ and $KAlO_2$). The 5% error which was used as convergence threshold for plane wave cut-off is shown as a horizontal dashed line.

1.3 Definition of Error

For all the comparisons between experimental and DFT-calculated parameters, we define the Mean Absolute Error (MAE)

$$\mathrm{MAE} = \frac{1}{k}\Sigma_{i=1}^{k}|x_i^{DFT} - x_i^{Ref}|, \tag{5}$$

that can also be expressed as a percentage

$$\mathrm{MAE}(\%) = \frac{100}{k}\Sigma_{i=1}^{k}\frac{|x_i^{DFT} - x_i^{Ref}|}{x_i^{Ref}}. \tag{6}$$

These formula can be applied for calculating the MAE of the observables C_Q and η as described in the main text or for the principle components V_{ii} of the EFG tensor (Figs. S3 and S4). The MAE discussed here describes the deviation of the DFT results with respect to the linear regression fit (Ref = lin. regression). he accuracy of the DFT results with respect to experimental literature values is evaluated with the parameters of the linear fit.

For the correlation of the direction cosines in Figure 3, we calculate the error of each DFT tensor with the following formula

$$\mathrm{MAE}(\%) = \frac{100}{9}\Sigma_{i=1}^{i=3}\Sigma_{j=1}^{j=3}\frac{|\mu_{ij}^{DFT} - \mu_{ij}^{Ref}|}{\mu_{ij}^{Ref}}, \tag{7}$$

where Ref corresponds to the experimental direction cosines taken from literature.

2 Pseudopotential Modifications

2.1 Effect of a Hard Pseudopotential on ^{27}Al

For the Al compounds, a hard PP with an ionic charge of 11 was tested by using the following string for the Al atom:

2|1.2|23|26|29|20U:21U:30:31(qc=8).

The calculated quadrupolar observables are listed in S3 and show a slightly worse correlation to experimental values than the default CASTEP PP, with a MAE of 1.01 MHz and 0.11 for C_Q and η_Q, respectively (while the default PP gives a MAE of 0.84 MHz and 0.11). The impact of the PP is minor, since the hard PP does not introduce new features that drastically modify the electronic density in the core region.

2.2 Effect of the Core Radius on ^{7}Li

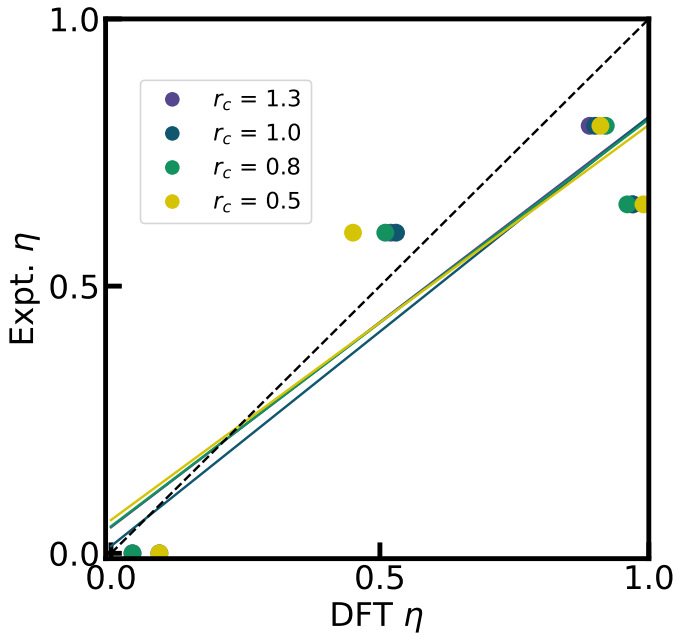

Fig. S2 Test with harder CASTEP PP. By changing the core radius r_c for the Li PP in CASTEP (default $r_c = 1.0$), we demonstrate the effect of a smaller Li pseudozised core region on the simulated η for three Li compounds ($LiIO_3$ [96], Li_2CO_3 [21], $Li_2B_4O_7$ [87], LiB_3O_5 [41]), with PBE, fixed cell geometries, and supercells. The dashed diagonal line indicates the limit of ideal correlation.

In order to test the impact of the size of the PP core region for ^{7}Li, a set of three modified PPs was created by changing only the parameter related to the core radius r_c and the energy cut-off for the PP testing (qc). The strings passed to the otf PP generator are summarized in S2.

Table S2 ^{27}Al Castep strings used for creating each PP for the core radius effect test

Core radius	PP string
1.3	Li 1|1.3|14|16|18|10U:20(qc=7)
1.0 (default)	Li 1|1.0|14|16|18|10U:20(qc=7)
0.8	Li 1|0.8|14|16|18|10U:20(qc=14)
0.5	Li 1|0.5|14|16|18|10U:20(qc=18)

3 Tabulated Results

If the literature reference proposed different crystallographic phases of the studied compound, we chose the phase stable at room temperature. Similarly, we find several cases in the literature of a temperature-dependent C_Q value. These are $LiKSO_4$ [86], $LiNbO_3$ [94], and $LiNH_4SO_4$ [42]. We selected the C_Q value at room temperature for comparison with the DFT-calculated C_Q values. On the one hand, all other C_Q values were taken at room temperature, and on the other hand, the **fixed cell** geometries used are based on experimental lattice constants derived at room temperature.

Table S3 Summary of simulated and experimental ^{27}Al C_Q and η. The simulations are conducted with CASTEP and Quantum ESPRESSO (QE) using PBE, fixed cell geometry, and unit cells. The CASTEP calculations are conducted either with the default Li PP (C19) or with the hard Li PP. QE simulations are based on the Quantum ESPRESSO default PP. The experimental values are taken from literature. The source of the experimental input structure (empir.) is given in the column Chemical formula. The compounds are sorted by Group 1, Group 2, and compounds, for which the crystallographic sited could not be assigned unambiguously. [a] For these cells, the quadrupolar observables cannot unambigously assigned to their respective crystallographic sites, so we report the theoretical calculated value for each position and omit them in the reference scale. [b] Results not available because of the lack of a GIPAW-compatible PP for V. [133]

Chemical formula	Unit cell volume / Å^3	C19 C_Q /MHz	C19 η_Q	Hard C_Q /MHz	Hard η_Q	QE C_Q /MHz	QE η_Q	Reference C_Q /MHz	Reference η_Q
α-Al_2O_3 [site 1] [75]	85.02	2.33	0.00	2.06	0.00	2.17	0.00	2.38 [78]	0 [78]
α-Al_2O_3 [site 2] [75]	85.02	2.33	0.00	2.06	0.00	2.17	0.00	2.40 [78]	0.05 [78]
θ-Al_2O_3 [site 1] [75]	93.69	12.89	0.83	12.13	0.53	12.12	0.51	6.4 [98]	0.65 [98]
θ-Al_2O_3 [site 2] [75]	93.69	4.53	0.03	4.51	0.03	4.44	0.65	3.5 [98]	0 [98]
β-$NaAlO_2$ [75]	197.67	1.99	0.74	2.07	0.73	1.87	0.74	1.4 [134]	0.5 [134]
$MgAl_2O_4$ [75]	131.91	3.69	0.00	3.09	0.00	3.23	0.00	3.73 [92]	0.5 [92]
$KAlO_2$ [75]	918.04	1.54	0.73	1.48	0.86	1.60	0.89	1.1 [134]	0.7 [134]
$CaAl_4O_7$ [75] [site 1]	297.54	6.56	0.74	6.17	0.76	6.14	0.73	6.3 [80]	0.9 [80]
$CaAl_4O_7$ [75] [site 2]	297.54	9.28	0.78	9.27	0.78	8.78	0.78	9.5 [80]	0.82 [80]
cristobalite-$AlPO_4$ [82]	176.54	1.48	0.47	2.46	0.37	2.10	0.46	1.2 [77,135]	0.75 [77,135]
tridymite-$AlPO_4$ [75]	208.82	0.75	0.80	0.75	0.81			0.75 [135]	0.95 [135]
quartz-$AlPO_4$ [83]	231.77	4.29	0.51	4.71	0.25	3.92	0.50	4.2 [77]	0.35 [77]
$Na_5Al_3F_{14}$ [84]	511.71	6.78	0.18	6.28	0.14	7.16	0.14	8 [136]	0.13 [136]
Al_4C_3 [site 1] [85]	80.16	13.34	0.00	13.35	0.00	11.98	0.00	15.58 [76]	0 [76]
Al_4C_3 [site 2] [85]	80.16	17.50	0.00	17.50	0.00	17.64	0.00	15.83 [76]	0 [76]
Al_2SiO_5 [site 1] [43,74] [site 1]	340.97	15.33	0.17	14.28	0.05	14.34	0.16	15.26 [43]	0.1 [43]
Al_2SiO_5 [site 2] [43,74] [site 2]	340.97	5.47	0.67	6.47	0.66	4.97	0.72	5.83 [43]	0.67 [43]
γ-$LiAlO_2$ [74]	167.45	3.40	0.73	3.27	0.69	3.23	0.79	3.33 [109]	0.66 [109]
$AlVO_4$ [site 1] [75] [a]	426.63	2.02	0.88	1.99	0.66	[b]	[b]	1.64 [79]	0.3 [79]
$AlVO_4$ [site 2] [75] [a]	426.63	6.75	0.12	6.27	0.09	[b]	[b]	6.73 [79]	0.42 [79]
$AlVO_4$ [site 3] [75] [a]	426.63	5.45	0.34	5.37	0.37	[b]	[b]	5.88 [79]	0.58 [79]
κ-Al_2O_3 [site 1] [75] [a]	361.30	8.3	0.75	8.3	0.75	7.70	0.76	5.07 [78,81]	0.3 [78,81]
κ-Al_2O_3 [site 2] [75] [a]	361.30	10.06	0.46	10.06	0.46	9.49	0.46	3.33 [81] [78]	-
κ-Al_2O_3 [site 3] [75] [a]	361.30	8.11	0.95	8.11	0.95	7.70	0.76	10 [81] [78]	-
κ-Al_2O_3 [site 4] [75] [a]	361.30	7.74	0.49	7.74	0.49	9.49	0.46	5.67 [81] [78]	-

Table S4 Summary of ^{7}Li C_Q and η calculated with CASTEP and Quantum Espresso for each experimental reference Summary of simulated and experimental ^{7}Li C_Q and η. The simulations are conducted with CASTEP and Quantum ESPRESSO (QE) using PBE, fixed cell geometry, and default PP. The values calculated with CASTEP are based on either unit cells or supercells. The Quantum ESPRESSO values reported are for unit cells (no supercell effect detectable). The experimental values are taken from literature. The source of the experimental input structure (empir.) is given in the column Chemical formula. The compounds are sorted by Group 1 and Group 2. [a] The reference specifies that this spectrum does not exhibit any quadrupolar features, therefore we consider C_Q to be 0. [b] Results not available because of the lack of a GIPAW compatible PP for Sb, Ta, V, Cs and I. [c] For these cells, the default structure from reference already consisted in a supercell containing multiple stoichiometric primitive cells. [d] $LiNH_4SO_4$ is relaxed with fixed cell and reduced symmetry tolerance (0.001 Å) to allow for an equilibration of the N-H bonds (see main text).

Chemical formula	Unit cell volume / Å^3	Supercell C_Q /kHz	Supercell η	Unit Cell C_Q /kHz	Unit cell η_Q	QE C_Q /kHz	QE η_Q	Reference C_Q /kHz	Reference η_Q
LiOH [75]	104.09	111	0.00	70	0.00	359	0.00	110 [137]	0 [137]
$LiOH(H_2O)$ [75]	94.70	91	0.54	193	0.53	150	0.58	84 [137]	0.3 [137]
Li_2O_2 [site 1] [74]	63.11	51	0.07	280	0.01	8	0.00	0 [a 88]	-
Li_2O_2 [site 2] [74]	63.11	24	0.16	280	0.01	8	0.00	0 [a 88]	-
Li_2O_2 [avg.] [74]	63.11	33	0.11	280	0.01	8	0.00	0 [a 88]	-
Li_3N [75] [site 1]	43.50	661	0.01	690	0.00	510	0.00	582 ±2 [112]	-
Li_3N [75] [site 2]	43.50	302	0.03	272	0.00	87	0.00	295 ±2 [112]	-
Li_3P [74] [site 1]	116.35	255	0.01	150	0.01	142	0.64	68.5 ±3 [90]	-
Li_3P [74] [site 2]	116.35	77	0.04	210	0	142	0.64	16 [90]	-
Li_3Sb [74] [site 1]	70.09	204	0.00	152	0.00	[b]	[b]	75.2 ±3 [90]	-
Li_3Sb [74] [site 2]	70.09	54	0.00	106	0.00	[b]	[b]	18 ±1.3 [90]	-
Li_2CO_3 [21]	228.90	87	0.90	99	0.93	89	0.6	70 ±10 [21]	0.80 ±0.05 [21]
$LiNO_3$ [74]	148.20	64	0.00	130	0.00	49	0.00	39.2 [137]	0.0 [137]
$Li_2SO_4(H_2O)$ [74] [site 1]	215.35	51	0.77	71	0.58	5	0.87	46 [89]	-
$Li_2SO_4(H_2O)$ [74] [site 2]	215.35	72	0.21	79	0.36	49	0.21	70 [89]	-
$LiIO_3$ [74]	99.65	23	0.08	9	0.09	[b]	[b]	**36.4 ±0.5** [96], 45.2 [137]	0 [137 96]
$LiPS_3$ [74]	413.49	139	0.65	141	0.68	142	0.63	100 [93]	-
Li_3PS_4 [74]	159.51	37	0.22	54	0.73	53	0.95	30 [93]	-
$Li_4P_2S_6$ [74]	423.36	62	0.03	186	0.00	19	0.03	20 [93]	-
Li_2ZrO_3 [site 1] [74]	241.51	115	0.06	[c]	[c]	176	0	108 [137]	0 [137]
Li_2ZrO_3 [site 2] [74]	241.51	61	0.07	[c]	[c]	35	0.7	65.6 [137]	0 [137]
$LiTaO_3$ [74]	105.12	77	0.00	77	0.00	[b]	[b]	85 [138]	0 [138]
$KLiSO_4$ [139]	207.47	26	0.00	26	0.00	22.3	0.00	25 ±1 [140]	0.15 ±0.01 [140]
$LiTi_2(PO_4)_3$ [74]	935.81	33	0.00	36	0.00	79	0.00	37 [141]	0 [141]
$LiNbO_3$ [74]	429.06	53	0.00	55	0.00	54	0.00	**53.8 ±0.5** [94], 53.3 ±0.5 [94]	0 [94 96]
$LiCsB_6O_{10}$ [74]	1030.85	205	0.00	[c]	[c]	[b]	[b]	180 ±2 [95]	0 [95]
$Li_2B_4O_7$ [75]	466.65	132	0.97	[c]	[c]	119	0.66	104.5 [87]	0.65 [87]
LiB_3O_5 [41]	318.68	192	0.54	203	0.53	210	0.34	143 ±1 [41]	0.6 ±0.1 [41]
γ-$LiAlO_2$ [74]	31.80	138	0.63	159	0.62	135	0.02	115.1 ±0.6 [97]	0.69 ±0.01 [97]
$LiNH_4SO_4$ [d 75]	423.46	44	0.94	58	0.77	62	0.53	25 [42]	0.22 [42]

Table S5 EFG eigenvalues V_{ii} for ^{7}Li as found in literature and simulated with CASTEP, PBE, fixed cell geometry, default PP, and 2x2x2 supercells

Chemical formula	V_{xx}	DFT V_{xx}	V_{yy}	DFT V_{yy}	V_{zz}	DFT V_{zz}
$LiNbO_3$ [94]	0.038	0.033	0.038	0.033	0.076	0.062
$LiCsB_6O_{10}$ [95]	0.124	0.109	0.124	0.109	0.248	0.217
$Li_2B_4O_7$ [87]	0.025	0.002	0.119	0.138	0.144	0.140
LiB_3O_5 [41]	0.039	0.047	0.158	0.156	0.197	0.204

4 EFG Principal Components Correlation

For all experimental references which report both C_Q and η it is possible to extract the principal components (eigenvalues) of the EFG tensor from the relations Eqs. 3, 4 and the zero trace of the EFG tensor. Unfortunately, for many references (as shown in Tables S3 and S4), η is not always extracted from the experimental spectra. Therefore, although reporting the principal components gives a more detailed insight into how well each individual direction of the tensor is reproduced, we focus our discussion in the main text to C_Q and η.

For both ^{27}Al and ^{7}Li, we find that the lowest MAE and the best agreement with experiment is to be found for V_{xx}, since it is defined as the smallest (absolute) eigenvalue. Correspondingly, V_{zz} yields the largest absolute error. In general, our results are consistent with the general trends observed for C_Q and η. For all principle components of ^{7}Li, DFT considerably and systematically overestimates V_{ii}. The notable outliers both for ^{27}Al and ^{7}Li correspond to the outliers discussed in the text (θ-Al_2O_3, Li_3P, and Li_3Sb).

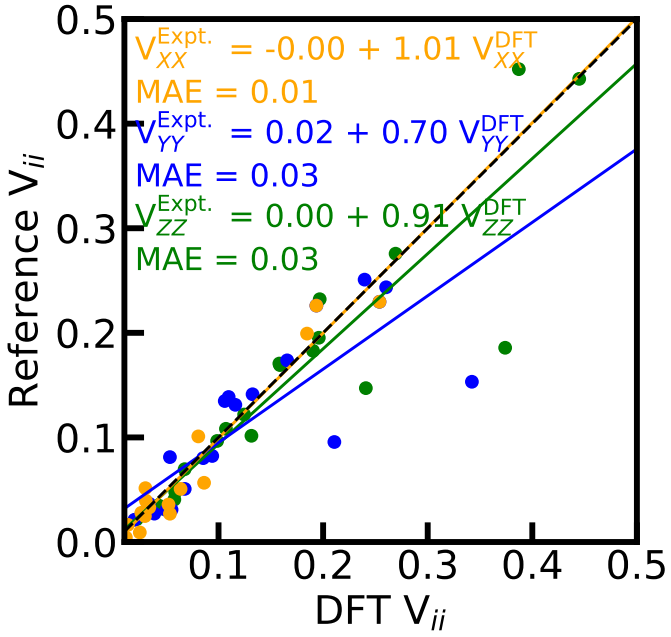

Fig. S3 Comparison of principal components V_{xx},V_{yy}, and V_{zz} derived from experimentally available C_Q and η with DFT calculations for ^{27}Al. DFT calculated values are derived with CASTEP, PBE, fixed cell structures, default PP, and unit cells.

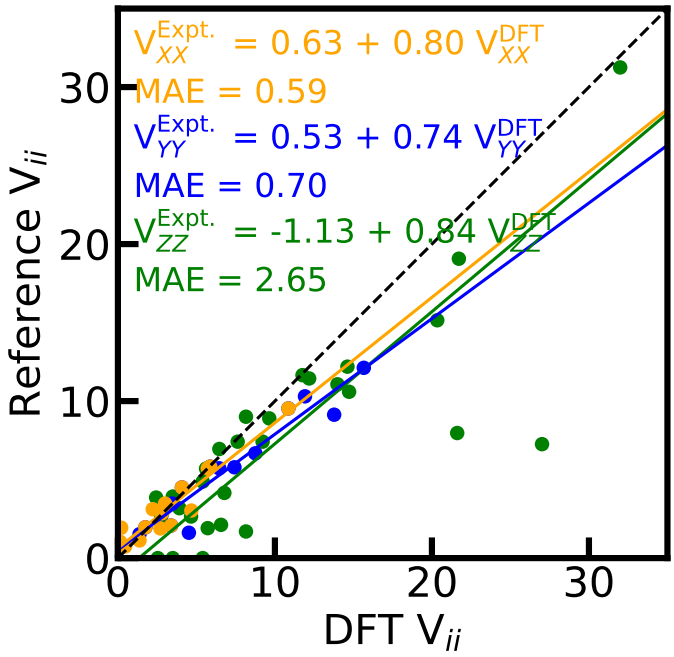

Fig. S4 Comparison of principal components V_{xx},V_{yy}, and V_{zz} derived from experimentally available C_Q and η with DFT calculations for ^{7}Li. DFT calculated values are derived with CASTEP, PBE, fixed cell structures, default PP, and 2×2×2 supercells.